



Received: October 26, 2016
Revised: November 9, 2016
Accepted: November 11, 2016

Corresponding author

Masaki Ishida, MD, PhD
Department of Radiology,
Mie University Hospital,
2-174 Edobashi,
Tsu 5148507, Japan
Tel: 81-59-231-5029
Fax: 81-59-232-8066
E-mail: mishida@clin.medic.mie-u.ac.jp

Cardiac MR Assessment of Coronary Arteries

Ahmed Hamdy, Masaki Ishida, Hajime Sakuma

Department of Radiology, Mie University Hospital, Tsu, Japan

Imaging of coronary arteries with magnetic resonance has undergone undeniable progress during the past two decades. Although coronary computed tomography angiography detects coronary artery disease (CAD) with excellent diagnostic accuracy, the inevitable exposure to ionizing radiation and iodinated contrast administration make it less appealing in certain patient populations. Coronary magnetic resonance angiography (MRA) is now performed mostly as a whole heart, free breathing, three-dimensional study. Several factors influence quality and speed of the scan, including use of the appropriate pulse sequence according to the strength of the magnetic field, cardiac and respiratory gating, preparation pulses, multi-channel cardiac coils, parallel imaging, and contrast material injection. The use of coronary MRA is well established in coronary artery anomalies and aneurysms. While diagnostic performance has also improved markedly for the detection of CAD, coronary MRA is not yet a routine clinical study. However, coronary MRA is expected to play a major role in the near future due to continuous research and technical achievements.

Key words Heart · Coronary vessels · Magnetic resonance angiography · Coronary artery disease.

INTRODUCTION

Coronary MRA; Achilles heel of cardiac MRI?

Although cardiac magnetic resonance (CMR) imaging is now regarded as the gold standard for assessment of cardiac function, morphology, myocardial viability, and tissue characterization, its role in coronary arteries assessment has been considered premature and vulnerable. In contrast, coronary computed tomography angiography (CCTA) has taken the lead in the field of non-invasive imaging of coronary arteries and has become a trustworthy gate-keeper for invasive catheterization [1]. CCTA, however, is not flawless. The technique entails inevitable exposure to ionizing radiation that—despite new technologies that allow for ultra-low radiation doses—still cannot be ignored in children, young adult patients, and those who are in need for serial CT examinations. In addition, CCTA is not suitable for patients whose renal problems preclude the administration of iodinated contrast material. Coronary magnetic resonance angiography (MRA), on the other hand, is a non-ionizing radiation modality that can be performed even without contrast injection and is of particular benefit in patients with heavily calcified coronary arteries (Fig. 1). A coronary MRA study is tech-

nically challenged by the small size, tortuous courses and complex motion of coronary arteries during cardiac and respiratory cycles, as well as the need for whole coronary tree coverage with high spatial resolution. Some of these challenges have been resolved by technical advances that have significantly improved image quality and overall diagnostic performance of coronary MRA in patients with coronary artery disease (CAD); however, challenges remain. In this review, we will try to summarize various coronary MRA imaging strategies and describe the current status of coronary MRA in clinical practice.

CORONARY MRA TECHNIQUES: PAST, PRESENT, AND FUTURE

The past

The earliest attempts at coronary imaging with MRI used a breath-hold, two-dimensional (2D), coronary segmented k-space gradient-echo technique [2-4]. Despite being relatively easy to implement, breath-hold 2D coronary MRA was limited by suboptimal signal-to-noise ratio (SNR), slice misregistration due to inconsistent diaphragm positions between breath-holds, high operator dependency, and patient fatigue from repeated breath-holds. The 2D imaging technique later evolved into a three-dimensional (3D) gradient echo coronary MRA that improved SNR and slice registration, but still used the breath-hold

© This is an Open Access article distributed under the terms of the Creative Commons Attribution Non-Commercial License (<http://creativecommons.org/licenses/by-nc/3.0>) which permits unrestricted non-commercial use, distribution, and reproduction in any medium, provided the original work is properly cited.

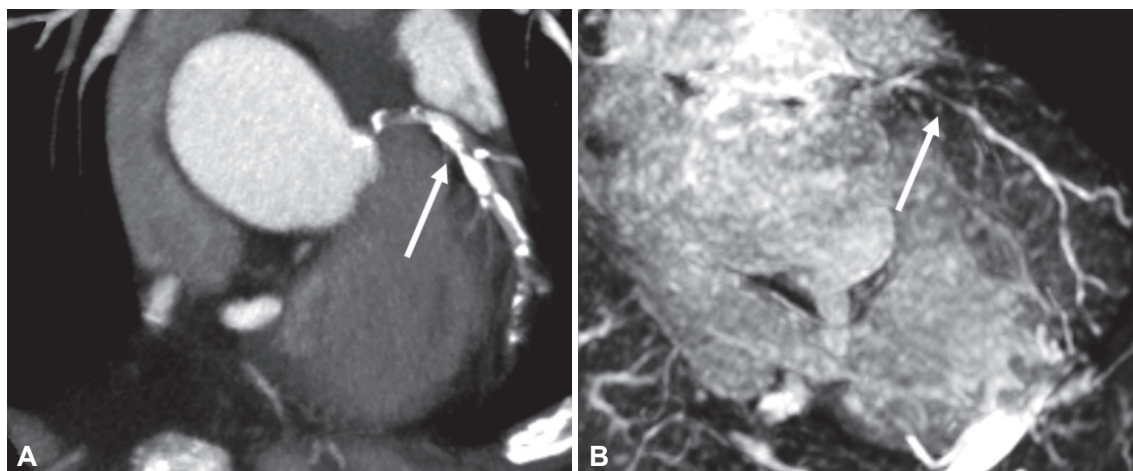


Fig. 1. (A) Reformatted coronary CT angiography showing a heavily calcified proximal LAD plaque that prevented assessment of that segment (arrow). Coronary MRA of the same subject revealed significant stenosis in the region of the heavy calcification (B, arrow) that was confirmed on X-ray coronary angiography (not shown). LAD: left anterior descending, MRA: magnetic resonance angiography.

method. Wielopolski et al. [5,6] used a breath-hold, 3D coronary MRA with double oblique volume-targeted technique in which each coronary segment was imaged during a single end-expiratory breath-hold with a total of about 13 breath holds for coverage of all major coronary arteries. van Geuns et al. [7] assessed the diagnostic accuracy of this approach and reported that 69% of segments were assessable, with sensitivity and specificity of 92% and 68%, respectively, for the detection of >50% luminal stenosis. One advantage of the breath-hold technique is that it allows for imaging of coronary arteries during the first pass of extracellular MR contrast media (e.g., Gd-DTPA), which rapidly diffuses from the intravascular space to the interstitial space after intravenous administration [8-11]. Regenfus et al. [11] obtained breath-hold 3D coronary MRA immediately after injecting extracellular MR contrast agent at a flow rate of 1 ml/s and reported 94% sensitivity and 57% specificity for detecting significant CAD. However, the short imaging time of the breath-hold technique is a tradeoff with reduced spatial resolution and 3D volume coverage. Also, breath-holding does not eliminate motion of the diaphragm as it continues to drift during breath-holding, which causes significant blurring on breath-hold 3D coronary MRA [12]. In addition, the impaired cardiopulmonary reserve in many of the patients referred for the procedure is yet another limitation.

The present

Free-breathing 3D MRA is currently the most widely used MRI technique for coronary imaging. 3D imaging allows for better SNR slice registration and greater volume coverage compared to 2D imaging. Free breathing was also implemented to avoid the drawbacks of breath holding. The superior image quality of free-breathing 3D coronary MRA can be achieved by applying several strategies including respiratory motion correc-

tion, cardiac gating, acquisition and preparation pulse sequences, parallel imaging, as well as contrast administration and magnetic field strength.

Respiratory gating

Initial trials for free breathing coronary MRA used respiratory monitoring belts that, despite improved resolution and coronary alignment, could not eliminate respiratory motion artifacts and blurring [13]. The introduction of respiratory navigators (MR signals that measure the position of the right lung-diaphragm interface) markedly improved image quality of free-breathing MRA. Respiratory navigator gating was initially performed in a retrospective fashion in which only images within a gating window were used to reconstruct coronary MRA [14-17]. This was replaced with real-time prospective navigation, where both navigator and coronary imaging data are acquired at the same time during the cardiac cycle [18,19]. The lung-diaphragm interface must lie within a predefined acceptance window (typically ± 2.5 mm) at end-expiration for the image data to be accepted, or it is rejected and acquisition is repeated in next cardiac cycles until collection of all necessary data in k-space.

Obviously, this technique is disadvantageous in terms of increased acquisition time and inappropriateness in patients with irregular breathing patterns and persistent diaphragmatic position drift. The use of multi-channel cardiac coils with higher parallel imaging factor can be a partial solution for this issue, as the short scanning time can reduce undesirable breathing irregularities. By applying this strategy, Nagata et al. [20] significantly reduced the coronary MRA scanning time from 12.3 ± 4.2 min with 5-channel coils to 6.3 ± 2.2 min using 32-channel coils. Consequently, the reduced imaging time increased the MRA acquisition success rate (100%) and maintained image quality. Another strategy is to use abdominal belts that restrict dia-

phragmatic position drifting. Ishida et al. [21] reported that this technique significantly improved scan efficiency and image quality in both UK and Japanese patients. When used in combination with 32-channel coils, Nagata et al. [20] reported 86% sensitivity and 93% specificity of 1.5 T whole heart coronary MRA for detecting significant CAD on a vessel-based analysis.

Cardiac gating

Unlike X-ray coronary angiography, in which time per image frame is less than 20 milliseconds, electrocardiographic (ECG) gating is indispensable in coronary MRA in order to enable imaging of coronary arteries while they are most static during the cardiac cycle. The acquisition window and the optimal delay after the R wave, however, are not fixed for all patients and are affected not only by the heart rate, but also by patient hemodynamics. Consequently, a subject-specific acquisition window needs to be determined. For this purpose, Wang et al. [22] proposed an ECG-triggered M-mode navigator-echo technique to define the optimal period of minimal cardiac motion in the cardiac cycle. However, the currently most commonly used technique is to acquire high-temporal resolution cine MR images prior to coronary imaging and to visually track the right coronary artery (RCA) to determine the optimal trigger delay and acquisition window [23].

Another reason why free-breathing MRA prolongs scanning time is that it uses a narrow acquisition window to minimize cardiac motion artifacts. Again, a higher parallel imaging factor with the use of 32-channels coil could actually narrow the acquisition window of the MRA study in addition to its previously mentioned value in reducing the whole scan time. In the study by Nagata et al., [20] the use of 32-channel cardiac coils with a parallel imaging factor of 4 achieved a mean acquisition window of 84 ± 57 ms for diastolic acquisition and 48 ± 18 ms for systolic acquisition compared to 152 ± 67 ms and 98 ± 26 ms in a previous study using 5-channel cardiac coils. The success rate, image quality, and overall scan time were all substantially improved [24]. An even narrower acquisition window of less than 50 ms is essential in patients with a high heart rate in order to reduce motion artifacts on coronary MRA. As a rule of thumb, a narrow acquisition window of 30–50 ms is recommended to obtain sharp coronary MRA, even in patients with low heart rate.

Acquisition pulse sequence and magnetic field strength

Steady state free precession (SSFP) pulse sequences are currently used for 3D coronary MRA acquisition on 1.5 Tesla (1.5 T) MRI scanners after having replaced gradient echo sequences previously used in 2D and 3D MRA. SSFP provides higher blood signal intensity, reduced motion artifacts, and superior vessel sharpness that are further enhanced when used with an

optimized k-space sampling strategy such as radial sampling [25]. More importantly, the SSFP sequence is not dependent on in-flow effects and allows for whole heart coronary MRA acquisition. This allows visualization of the coronary tree with a single 3D scan, saves time, and is simple to plan. Moreover, the whole heart SSFP sequence allows for visualization of the distal coronary artery segments that were not easily assessed using the previous targeted double oblique technique. Using this method, we have demonstrated that more than 90% of distal coronary segments exhibited good to excellent image quality [20,24,26].

At higher magnetic field strength [i.e., 3 Tesla (3 T)], gradient echo sequences are generally preferred to SSFP for coronary MRA acquisition (Fig. 2). It is true that a stronger magnetic field means higher SNR, but this comes at the expense of increased magnetic field inhomogeneity and specific adsorption rate, ultimately causing increased off-resonance. This is disadvantageous for coronary MRA using SSFP acquisition because of its higher susceptibility to inhomogeneity of magnetic field and the need for higher flip angles to achieve sufficient blood contrast. Coronary MRA acquisition using 3 T was shown to be feasible in humans by Stuber et al. [27]. A combination of gradient echo whole heart coronary MRA and gadolinium contrast administration at 3 T produces high-resolution coronary MRA with significantly improved image quality and diagnostic accuracy compared with those at 1.5 T [28,29].

Recently, Gharib et al. [30] demonstrated the feasibility of 350 μ m spatial resolution coronary MRA at 3 T in humans. This high resolution of volume-targeted MRA is similar to that of multi-detector CT. Despite having lower SNR, the improved sharpness of the images resulted in better quality and better qualitative assessment. One disadvantage of the technique is that it requires at least 9 minutes of scan time per vessel, which can be intolerable to some patients.

Preparation pulses for ensuring sufficient image contrast

Preparation pulse sequences are used to suppress signals from structures surrounding coronary arteries, namely epicardial fat and myocardium, to ensure that maximal coronary arterial blood contrast is achieved during imaging. For pericardial fat suppression, the spectral presaturation with inversion recovery pulse sequence is widely preferred because of its selective fat suppression and high SNR. The short tau inversion recovery sequence is also used, particularly in contrast-enhanced studies. Recently, researchers have developed a highly resolved, T1-weighted (TIW), dual-echo Dixon approach and reported significantly improved image quality ($p < 0.000001$) compared to conventional fat-suppression techniques [31]. This approach permits additional assessment of intra- and extra-myocardial fat deposits that gained interest in a number of new clinical studies.

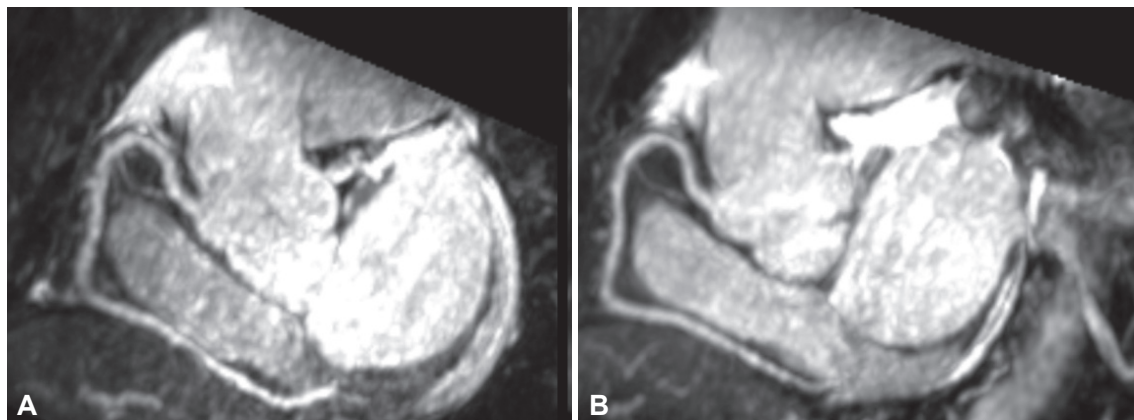


Fig. 2. Free breathing, whole heart, coronary MRA study acquired with the steady-state free-precession technique at 1.5 T (A) and with a gradient-echo sequence at 3 T (B) in the same subject with non-contrast, 32-channel coils, T2 and spectral fat-saturation inversion recovery pre-pulses. Slightly but not significantly better image quality can be noted in the 3 T gradient-echo image. MRA: magnetic resonance angiography.

As for the myocardium, a T2-weighted magnetization preparation pulse is used to suppress the myocardial signal [18]. The T2 preparation pulse additionally suppresses venous blood signal in the epicardial veins, taking advantage of the substantially shorter T2 relaxation time of deoxygenated venous blood compared to that of oxygenated arterial blood. Recently, Soleimani-fard et al. [32] introduced a spatially selective T2 preparation pulse where the position of the T2Prep slab can be freely adjusted to avoid covering the ventricular blood-pool and hence enable acquisition of better SNR.

Parallel imaging techniques

The aim of parallel imaging is to increase scanning speed, which means higher study success rate and better patient tolerance. Sensitivity encoding, a parallel imaging technique in image space, along with generalized autocalibrating partially parallel acquisition and simultaneous acquisition of spatial harmonics, which provide parallel imaging in k-space, are now widely used to reduce the scan time of 3D coronary MRA in clinical settings [33-35]. However, parallel imaging comes at the cost of reduced SNR. That said, the “need for speed” during coronary imaging needs to be appropriately weighted against image quality. Availability of 3 T MRI units and multi-channel cardiac coils has made it possible to use parallel imaging techniques while maintaining good SNR.

Contrast medium

Contrast material administration is another strategy for enhancing coronary artery visualization through its T1 shortening effect. This means that blood signal intensity is determined by its T1 relaxation time rather than its in-flow effect, which enables acquisition of 3D gradient echo coronary MRA with large 3D volume coverage. Contrast media that can be used are extracellular, intravascular, or slightly albumin-binding. Unlike

the more widely used extracellular contrast material whose T1 shortening of the coronary arterial blood is only maintained during the first pass following administration, intravascular contrast material remains in the blood pool for a longer time and exhibits greater T1 shortening effects [8,9]. Raman et al. [29] compared gadofosveset (0.03 mmol/kg), an intravascular contrast agent, to Gd-BOPTA (0.1 mmol/kg), an extracellular agent, for free-breathing 3D coronary MRA and reported that use of the intravascular contrast agent performed as well as, or slightly better than, the extracellular contrast agent at 3 T. Slightly albumin-binding contrast medium combines the benefits of both extracellular and intravascular agents as it remains in the blood for a relatively prolonged time with greater T1 shortening effect while maintaining late enhancement abilities [36,37]. Several studies have agreed on the ability of intravascular or slightly albumin-binding agents to improve arterial contrast on 3D gradient echo coronary MRA, particularly when used with an inversion-recovery pre-pulse [38-42].

Future perspectives in coronary MRA techniques

As previously explained, the currently used respiratory navigation technique is one reason for prolonged coronary MRA scanning time. In recent years, there has been extensive work toward developing sophisticated respiratory motion correction techniques that can reduce examination time by acquiring data throughout most or all of the respiratory cycle. One of these techniques is self-gating navigation MRA that allows for up to 100% scan efficiency increase as all data segments are used for the final image reconstruction [43]. The technique was further developed to iterative self-navigation that does not require the choice of a respiratory reference position [44]. The image-based navigator technique is another method that uses a spatially encoded, low-resolution, 2D image acquired just before the acquisition of k-space data to correct the high-resolution data [45,46].

The method was reported to increase scan efficiency without compromising image quality. A 3D version of the technique was also described [47].

Recently, respiratory binning techniques with 3D affine motion correction were described to adapt to the more complex 3D motion. In respiratory binning, the respiratory signal is distributed throughout the breathing cycle like “bins” and then corrected to a reference position using the low-resolution images [48]. In a more sophisticated approach, respiratory binning was superimposed on self-gating and image-based navigations and proved to be a useful strategy to significantly reduce scan time and improve motion correction [49-51].

Compressed sensing is a new image reconstruction technique that uses incoherently undersampled k-space data for accelerated acquisitions [52]. Akçakaya et al. [53] performed a head-to-head comparison of highly accelerated, submillimeter, whole-heart coronary MRA and parallel imaging techniques. The image quality and SNR of the compressed sensing images were significantly higher than those of parallel imaging.

Recent advances have also lead to the development of four-dimensional (4D) whole-heart coronary MRA. Free running mode with retrospective cardiac gating and retrospective respiratory self-gating are used to produce 4D whole heart imaging, enabling simultaneous assessment of both coronary anatomy and ventricular function [54].

CLINICAL APPLICATIONS OF CORONARY MRA

The clinical indications of coronary MRA are currently limited to the detection and follow up of coronary artery anomalies,

ectasia, or aneurysms. In CAD, however, coronary MRA is not yet performed on a wide scale in the clinical setting.

Anomalous coronary arteries

Detection of coronary artery anomalies is important, particularly in vessels that have a so called “malignant course” where sudden death can be the result.

X-ray coronary angiography-other than being an invasive procedure involving ionizing radiation-lacks important data on the 3D path of the coronary artery. As is the case with CCTA, coronary MRA has been shown to have high sensitivity and specificity for detecting anomalous coronary arteries and for delineating their proximal courses [55-57] (Fig. 3). With the increasing availability of low-dose CT technology, lack of radiation exposure does not always justify the use of coronary MRA instead of CCTA. The choice between CCTA and coronary MRA should be made in each institution after considering the pros and cons of each modality (e.g., effective radiation dose by the CT machine employed, quality of coronary MRA images, patient tolerance and preferences).

Kawasaki disease

The prevalence of Kawasaki disease (KD) is highest among children of East Asian countries. Of these, Japan has the greatest prevalence; recently published statistics indicate that there are about 27000 patients with KD in Japan [58]. Incidence rates are increasing on an annual basis; (approximately 215 per 100000 per year in 2008 for children aged 0–4 years, 243 in 2011, and 308 in 2014, which is the highest recorded incidence so far). Coronary artery aneurysms are detected in 25% of untreated KD patients [59]. Serial assessment of aneurismal size is

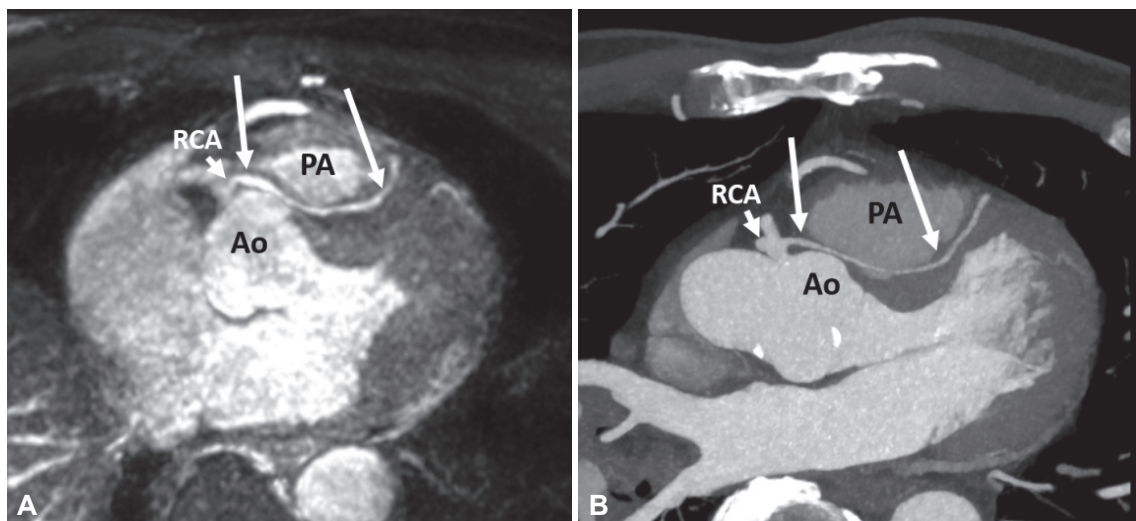


Fig. 3. Maximum-intensity projection images of whole-heart coronary MRA acquired with a gradient-echo sequence at 3 T (A) and reformat CT coronary angiography (B) in a young adult showing anomalous left anterior descending artery (arrows) that arises from the proximal segment of the right coronary artery (RCA) and runs in an inter-arterial course between the aorta (Ao) and main pulmonary artery (PA). Sufficient diagnostic data were obtained from the MRA study. MRA: magnetic resonance angiography.

important as it changes over time and is correlated with the risk of coronary artery thrombosis and stenosis. As is the case with coronary artery anomalies, X-ray coronary angiography and CCTA are not recommended for the young patient population. Assessment of coronary aneurysms in young children is classically performed using transthoracic echocardiography. However, as children grow, evaluation of coronary arteries becomes more difficult. Thanks to recent technical advances, coronary MRA can be used as an alternative to transthoracic echocardiography when image quality is insufficient [60] (Fig. 4). In one study, coronary MRA was reported to have excellent agreement with X-ray angiography for the diagnosis and quantitative analysis of coronary aneurysms [61].

Coronary artery disease

The diagnostic accuracy of coronary MRA for detecting CAD is chronologically linked to technical developments, which account for the considerable variation among coronary MRA studies. For example, the first multicenter study to assess free-breathing, navigator-gated, 3D gradient echo coronary

MRA reported a sensitivity of 93% but poor specificity of only 42% for detecting significant CAD [62]. The introduction of SSFP and free breathing approaches markedly improved diagnostic performance. Jahnke et al. [63] compared breath-hold to free-breathing 3D coronary MRA, both using SSFP and double oblique targeted volume acquisition techniques. Free-breathing was superior to breath-hold coronary MRA in terms of image quality, coronary artery segment assessment (79% vs. 45%), sensitivity, and specificity (72% and 92% by free-breathing approach vs. 63% and 82% by breath-hold approach). With introduction of the whole heart approach, the use of dedicated phased-array cardiac coils and the introduction of the concept of parallel imaging, even more promising results were obtained (Fig. 5). In our study of 131 patients, free breathing, SSFP, whole heart 3D coronary MRA was performed using a patient-specific acquisition window set either during systole or diastole, depending on the phase of minimal motion of the RCA on cine MR images. The success rate of MRA acquisition was 86% with 82% sensitivity, 90% specificity, 88% positive predictive value, and 86% negative predictive value for detecting significant

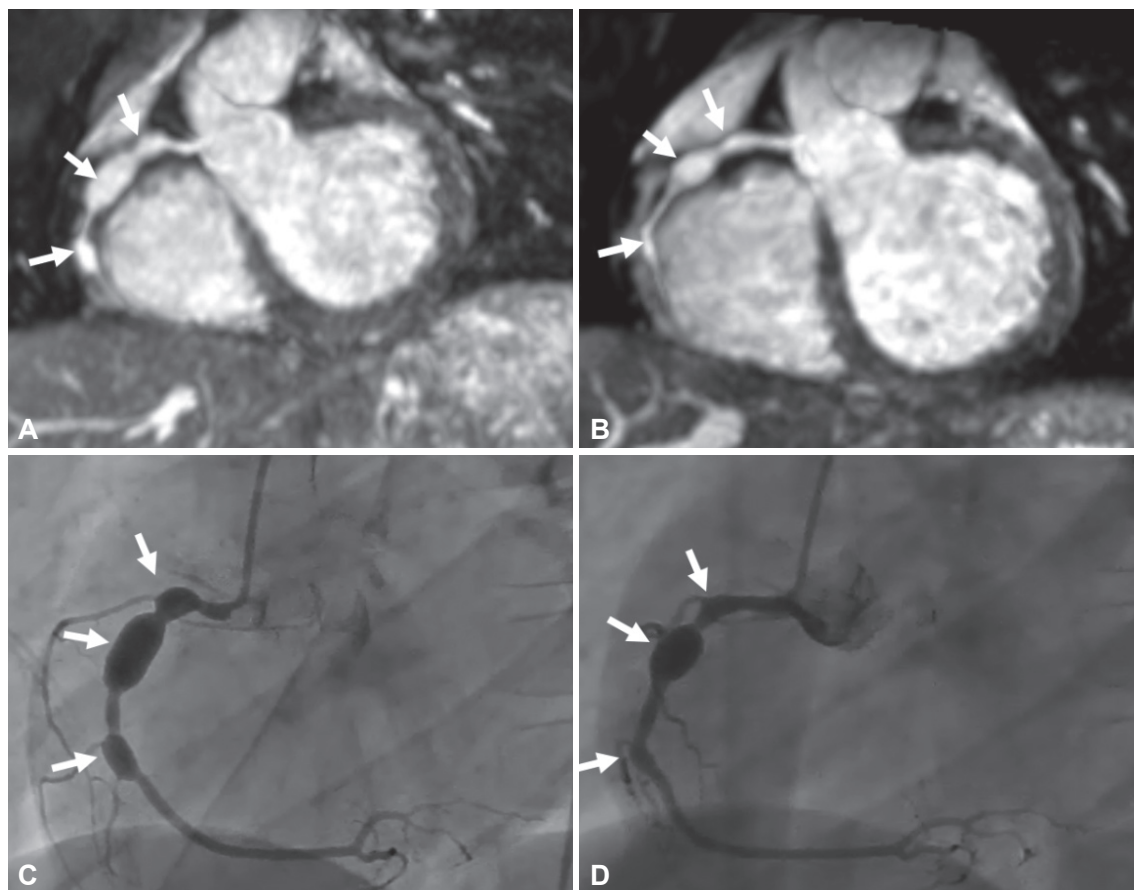


Fig. 4. A now 6-year-old child with right coronary artery (RCA) aneurysms secondary to Kawasaki disease. (A) Thin-slab maximum-intensity projection images of the initial whole-heart coronary MRA showed 3 RCA aneurysms. (B) On follow up MRA, all aneurysms showed significant reduction in size and change of morphology. (C and D) Corresponding X-ray coronary angiography shows the same changes. MRA: magnetic resonance angiography.

CAD [24]. A multicenter study showed that using 5-channel cardiac coils and a parallel imaging factor of 2 allowed detection of significant CAD with a sensitivity of 88%, specificity of 72%, and a negative predictive value of 88% [64]. This negative predictive value is similar to that of the CORE-64 CTA multicenter study [6], indicating that whole heart coronary MRA can effectively be used to rule out CAD. In the study by Nagata et al., [20] the combined use of 32-channel cardiac coils, parallel imaging factor of 4, and abdominal belt technique achieved 86% sensitivity, 93% specificity, 86% positive predictive value, 93% negative predictive value and 91% diagnostic accuracy in almost half of the imaging time of whole heart coronary MRA using 5-channel coils [24]. Higher magnetic field strength at 3 T MRI and contrast material administration achieve higher SNR of coronary MRA when a gradient echo technique is used. Yang et al. [42] acquired 3 T MRA with a gradient echo sequence and inversion recovery preparation during slow infusion of slightly al-

bumin-binding contrast medium. They reported 94% sensitivity and 82% specificity for detecting patients with >50% coronary stenosis. The same group conducted a second similar study but added 32-channels cardiac coils to their scanning protocol. They obtained diagnostic quality MRA images in 92% of patients with an average imaging time of 7.0 ± 1.8 minutes [42]. Moreover, the sensitivity, specificity, positive predictive value, and negative predictive value were 95.9, 86.5, 87.0, and 95.7%, respectively, indicating that the diagnostic performance of 3 T contrast-enhanced whole-heart coronary MRA approaches that of 64-slice CCTA [65].

Quantitative assessment of coronary MRA also proved to be diagnostically accurate. Yonezawa et al. [66] used the signal intensity profile along the vessel to develop a method for quantitative analysis of stenosis on coronary MRA. Using this method, coronary MRA had a sensitivity of 90% and a specificity of 80% for detecting >50% stenosis with excellent agreement with X-

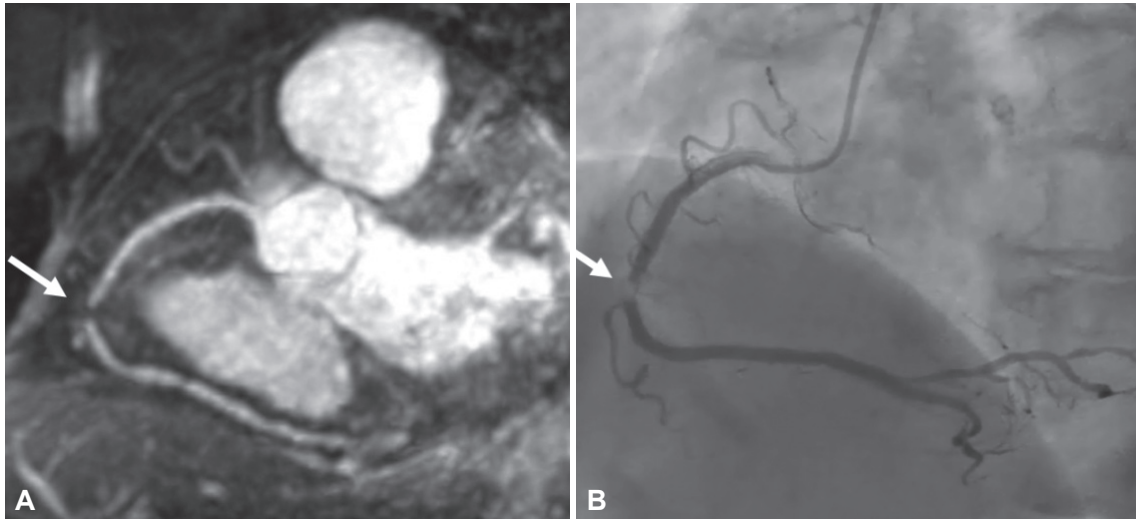


Fig. 5. Maximum-intensity projection images of whole-heart coronary MRA in an 88-year-old female with significant mid-RCA stenosis (arrowed) (A) that was confirmed on X-ray coronary angiography (B). MRA: magnetic resonance angiography, RCA: right coronary artery.

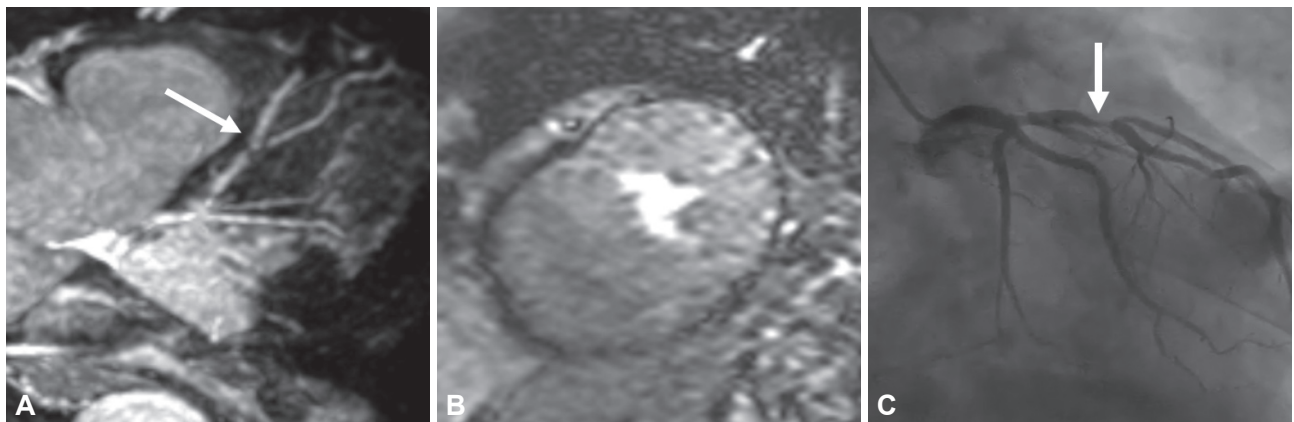


Fig. 6. (A) Coronary MRA in a 67-year-old man with chest pain revealed significant LAD stenosis just proximal to the origin of the first diagonal artery (arrow). (B) Stress perfusion MRI, however, did not detect stress-induced ischemia. (C) On X-ray angiography, significant (75%) stenosis was detected (arrow). MRA: magnetic resonance angiography, LAD: left anterior descending.

ray coronary angiography [correlation coefficient of 0.84 ($p < 0.001$)]. More recently, Kim et al. [67] investigated the relationship between signal intensity of coronary arteries with chronic total occlusion on coronary MRA and success rate of PCI. Areas of low or interrupted high signal showed a success rate of 72%, whereas areas of continuous high signal intensity were associated with 95% success rate, signifying its role as an independent predictor of PCI success (odds ratio, 8.20; $p = 0.042$).

In a comprehensive CMR protocol, combined use of stress perfusion MRI and coronary MRA should—at least theoretically—improve detection of obstructive CAD (Fig. 6). However, reports on the additive value of coronary MRA oppose this theory [68,69]. Sub-analysis of the recent multicenter prospective study (CE-MARC study) also found no significant additive value of coronary MRA [70]. On the other hand, Heer et al. [71] found different results when they adopted a more differentiated approach. In their algorithm, MRA was added only to low confidence results of stress perfusion CMR. The result was a significant increase in specificity (from 79.3% to 88.9%, $p = 0.008$) without worsening sensitivity (from 86.7% to 95.7%).

Data on prognostic performance of coronary MRA are scarce. In their study on 207 patients with suspected CAD, Yoon et al. [72] found that the presence of significant ($>50\%$) stenosis on coronary MRA was strongly associated with future cardiac death and major adverse cardiac events. Cox regression analysis showed that presence of significant stenosis on MRA was associated with >20 -fold hazard increase of all cardiac events.

Coronary artery wall imaging

The ability of non-contrast CMR to assess coronary wall thickness and positive remodeling has been investigated in patients with subclinical CAD, patients with type I diabetes, and in a multiethnic population cohort [73-75]. In addition, non-contrast, TIW CMR was able to directly visualize thrombus in acute myocardial infarction and to detect the presence of coronary high-intensity plaques (HIPs), which correspond to positive remodeling and low-density plaques on CT [76,77]. Noguchi et al. [78] took a further step by demonstrating that HIPs identified by non-contrast T1W MRI were significantly associated with coronary events. The authors calculated the plaque-to-myocardium signal intensity ratio (PMR) for each coronary plaque. Interestingly, the presence of plaques with PMR of 1.4 was a significant independent predictor of coronary events [hazard ratio (HR): 3.96; 95% confidence interval (CI): 1.92 to 8.17; $p < 0.001$] compared with the presence of CAD (HR: 3.56; 95% CI: 1.76 to 7.20; $p < 0.001$) and other traditional risk factors. In another study by the same group, the ability of PMR to monitor therapy with statins was evaluated. In control subjects with CAD who were not treated with statin, PMR significantly increased after 12 months from baseline (from 1.22 to 1.49, a

19.2% increase; $p < 0.001$) but was significantly reduced in patients treated with statin (1.38 to 1.11, an 18.9% reduction; $p < 0.001$) [79]. A contrast-enhanced approach can also be used for plaque characterization with CMR. Studies using clinically approved extracellular contrast agents showed that uptake in the coronary artery wall is non-specific and could be associated with both atherosclerotic plaque composition and inflammation in patients with stable CAD or acute coronary syndrome [80,81]. Enhancement with newly developed albumin binding and iron oxide-based contrast agents is associated with increased endothelial permeability and thus can be used for coronary wall imaging [82-85].

CONCLUSION

Coronary MRA allows for non-invasive imaging of coronary arteries with no risk of exposure to ionizing radiation. Currently, the most popular technique for coronary MRA is free breathing, whole heart, 3D MRA with cardiac gating and respiratory navigation. SSFP pulse sequences are used in 1.5T MRI systems, while gradient echo sequences are used for 3 T MRA. Preparation pulses are needed for fat saturation and myocardial signal suppression. Contrast-enhanced MRA allows for more signal contrast of coronary arteries. Scanning time can be reduced with the use of parallel imaging and multi-channel cardiac coils. The main clinical indications for coronary MRA are detection and follow up of patients with coronary artery anomalies and aneurysms, e.g., KD. In CAD, diagnostic performance of coronary MRA has markedly increased in the past few years. With the help of more technical advances, coronary MRA could become a component of routine clinical practice for detecting CAD and plaque characterization.

Conflicts of Interest

The authors declare that they have no conflict of interest.

REFERENCES

1. Shaw LJ, Hausleiter J, Achenbach S, Al-Mallah M, Berman DS, Budoff MJ, et al. Coronary computed tomographic angiography as a gatekeeper to invasive diagnostic and surgical procedures: results from the multicenter CONFIRM (Coronary CT Angiography Evaluation for Clinical Outcomes: an International Multicenter) registry. *J Am Coll Cardiol* 2012;60:2103-2114.
2. Edelman RR, Manning WJ, Pearlman J, Li W. Human coronary arteries: projection angiograms reconstructed from breath-hold two-dimensional MR images. *Radiology* 1993;187:719-722.
3. Manning WJ, Li W, Edelman RR. A preliminary report comparing magnetic resonance coronary angiography with conventional angiography. *N Engl J Med* 1993;328:828-832.
4. Sakuma H, Caputo GR, Steffens JC, O'Sullivan M, Bourne MW, Shimakawa A, et al. Breath-hold MR cine angiography of coronary arteries in healthy volunteers: value of multiangle oblique imaging planes. *AJR Am J Roentgenol* 1994;163:533-537.
5. Wielopolski PA, Manning WJ, Edelman RR. Single breath-hold volumet-

- ric imaging of the heart using magnetization-prepared 3-dimensional segmented echo planar imaging. *J Magn Reson Imaging* 1995;5:403-409.
6. Wielopolski PA, van Geuns RJ, de Feyter PJ, Oudkerk M. Breath-hold coronary MR angiography with volume-targeted imaging. *Radiology* 1998;209:209-219.
 7. van Geuns RJ, Wielopolski PA, de Bruin HG, Rensing BJ, Hulshoff M, van Ooijen PM, et al. MR coronary angiography with breath-hold targeted volumes: preliminary clinical results. *Radiology* 2000;217:270-277.
 8. Goldfarb JW, Edelman RR. Coronary arteries: breath-hold, gadolinium-enhanced, three-dimensional MR angiography. *Radiology* 1998;206:830-834.
 9. Kessler W, Laub G, Achenbach S, Ropers D, Moshage W, Daniel WG. Coronary arteries: MR angiography with fast contrast-enhanced three-dimensional breath-hold imaging--initial experience. *Radiology* 1999;210:566-572.
 10. Li D, Carr JC, Shea SM, Zheng J, Deshpande VS, Wielopolski PA, et al. Coronary arteries: magnetization-prepared contrast-enhanced three-dimensional volume-targeted breath-hold MR angiography. *Radiology* 2001;219:270-277.
 11. Regenfus M, Ropers D, Achenbach S, Kessler W, Laub G, Daniel WG, et al. Noninvasive detection of coronary artery stenosis using contrast-enhanced three-dimensional breath-hold magnetic resonance coronary angiography. *J Am Coll Cardiol* 2000;36:44-50.
 12. Holland AE, Goldfarb JW, Edelman RR. Diaphragmatic and cardiac motion during suspended breathing: preliminary experience and implications for breath-hold MR imaging. *Radiology* 1998;209:483-489.
 13. Oshinski JN, Hofland L, Mukundan S Jr, Dixon WT, Parks WJ, Pettigrew RI. Two-dimensional coronary MR angiography without breath holding. *Radiology* 1996;201:737-743.
 14. Li D, Kaushikkar S, Haacke EM, Woodard PK, Dhawale PJ, Kroeker RM, et al. Coronary arteries: three-dimensional MR imaging with retrospective respiratory gating. *Radiology* 1996;201:857-863.
 15. McConnell MV, Khasgiwala VC, Savord BJ, Chen MH, Chuang ML, Edelman RR, et al. Comparison of respiratory suppression methods and navigator locations for MR coronary angiography. *AJR Am J Roentgenol* 1997;168:1369-1375.
 16. Post JC, van Rossum AC, Hofman MB, Valk J, Visser CA. Three-dimensional respiratory-gated MR angiography of coronary arteries: comparison with conventional coronary angiography. *AJR Am J Roentgenol* 1996;166:1399-1404.
 17. Woodard PK, Li D, Haacke EM, Dhawale PJ, Kaushikkar S, Barzilay B, et al. Detection of coronary stenoses on source and projection images using three-dimensional MR angiography with retrospective respiratory gating: preliminary experience. *AJR Am J Roentgenol* 1998;170:883-888.
 18. Botnar RM, Stuber M, Danias PG, Kissinger KV, Manning WJ. Improved coronary artery definition with T2-weighted, free-breathing, three-dimensional coronary MRA. *Circulation* 1999;99:3139-3148.
 19. Stuber M, Botnar RM, Danias PG, Kissinger KV, Manning WJ. Submillimeter three-dimensional coronary MR angiography with real-time navigator correction: comparison of navigator locations. *Radiology* 1999;212:579-587.
 20. Nagata M, Kato S, Kitagawa K, Ishida N, Nakajima H, Nakamori S, et al. Diagnostic accuracy of 1.5-T unenhanced whole-heart coronary MR angiography performed with 32-channel cardiac coils: initial single-center experience. *Radiology* 2011;259:384-392.
 21. Ishida M, Schuster A, Takase S, Morton G, Chiribiri A, Bigalke B, et al. Impact of an abdominal belt on breathing patterns and scan efficiency in whole-heart coronary magnetic resonance angiography: comparison between the UK and Japan. *J Cardiovasc Magn Reson* 2011;13:71.
 22. Wang Y, Vidan E, Bergman GW. Cardiac motion of coronary arteries: variability in the rest period and implications for coronary MR angiography. *Radiology* 1999;213:751-758.
 23. Plein S, Jones TR, Ridgway JP, Sivananthan MU. Three-dimensional coronary MR angiography performed with subject-specific cardiac acquisition windows and motion-adapted respiratory gating. *AJR Am J Roentgenol* 2003;180:505-512.
 24. Sakuma H, Ichikawa Y, Chino S, Hirano T, Makino K, Takeda K. Detection of coronary artery stenosis with whole-heart coronary magnetic resonance angiography. *J Am Coll Cardiol* 2006;48:1946-1950.
 25. Spuentrup E, Katoh M, Buecker A, Manning WJ, Schaeffter T, Nguyen TH, et al. Free-breathing 3D steady-state free precession coronary MR angiography with radial k-space sampling: comparison with cartesian k-space sampling and cartesian gradient-echo coronary MR angiography--pilot study. *Radiology* 2004;231:581-586.
 26. Sakuma H, Ichikawa Y, Suzawa N, Hirano T, Makino K, Koyama N, et al. Assessment of coronary arteries with total study time of less than 30 minutes by using whole-heart coronary MR angiography. *Radiology* 2005;237:316-321.
 27. Stuber M, Botnar RM, Fischer SE, Lamerichs R, Smink J, Harvey P, et al. Preliminary report on in vivo coronary MRA at 3 Tesla in humans. *Magn Reson Med* 2002;48:425-429.
 28. Prompona M, Cyran C, Nikolaou K, Bauner K, Reiser M, Huber A. Contrast-enhanced whole-heart coronary MRA using Gadofosveset 3.0 T versus 1.5 T. *Acad Radiol* 2010;17:862-870.
 29. Raman FS, Nacif MS, Cater G, Gai N, Jones J, Li D, et al. 3.0-T whole-heart coronary magnetic resonance angiography: comparison of gadobenate dimeglumine and gadofosveset trisodium. *Int J Cardiovasc Imaging* 2013;29:1085-1094.
 30. Gharib AM, Abd-Elmoniem KZ, Ho VB, Födi E, Herzka DA, Ohayon J, et al. The feasibility of 350 μm spatial resolution coronary magnetic resonance angiography at 3 T in humans. *Invest Radiol* 2012;47:339-345.
 31. Börnert P, Koken P, Nehrke K, Eggers H, Ostendorf P. Water/fat-resolved whole-heart Dixon coronary MRA: an initial comparison. *Magn Reson Med* 2014;71:156-163.
 32. Soleimanifard S, Schär M, Hays AG, Prince JL, Weiss RG, Stuber M. Spatially selective implementation of the adiabatic T2Prep sequence for magnetic resonance angiography of the coronary arteries. *Magn Reson Med* 2013;70:97-105.
 33. Griswold MA, Jakob PM, Heidemann RM, Nittka M, Jellus V, Wang J, et al. Generalized autocalibrating partially parallel acquisitions (GRAPPA). *Magn Reson Med* 2002;47:1202-1210.
 34. Pruessmann KP, Weiger M, Scheidegger MB, Boesiger P. SENSE: sensitivity encoding for fast MRI. *Magn Reson Med* 1999;42:952-962.
 35. Sodickson DK, Manning WJ. Simultaneous acquisition of spatial harmonics (SMASH): fast imaging with radiofrequency coil arrays. *Magn Reson Med* 1997;38:591-603.
 36. Krombach GA, Hahnen C, Lodemann KP, Krämer N, Schoth F, Neizel M, et al. Gd-BOPTA for assessment of myocardial viability on MRI: changes of T1 value and their impact on delayed enhancement. *Eur Radiol* 2009;19:2136-2146.
 37. Laurent S, Elst LV, Muller RN. Comparative study of the physicochemical properties of six clinical low molecular weight gadolinium contrast agents. *Contrast Media Mol Imaging* 2006;1:128-137.
 38. Herborn CU, Barkhausen J, Paetsch I, Hunold P, Mahler M, Shamsi K, et al. Coronary arteries: contrast-enhanced MR imaging with SH L 643A--experience in 12 volunteers. *Radiology* 2003;229:217-223.
 39. Klein C, Schalla S, Schnackenburg B, Bornstedt A, Hoffmann V, Fleck E, et al. Improvement of image quality of non-invasive coronary artery imaging with magnetic resonance by the use of the intravascular contrast agent Clariscan (NC100150 injection) in patients with coronary artery disease. *J Magn Reson Imaging* 2003;17:656-662.
 40. Paetsch I, Huber ME, Bornstedt A, Schnackenburg B, Boesiger P, Stuber M, et al. Improved three-dimensional free-breathing coronary magnetic resonance angiography using gadocoletic acid (B-22956) for intravascular contrast enhancement. *J Magn Reson Imaging* 2004;20:288-293.
 41. Stuber M, Botnar RM, Danias PG, McConnell MV, Kissinger KV, Yucel EK, et al. Contrast agent-enhanced, free-breathing, three-dimensional coronary magnetic resonance angiography. *J Magn Reson Imaging* 1999;10:790-799.
 42. Yang Q, Li K, Liu X, Bi X, Liu Z, An J, et al. Contrast-enhanced whole-

- heart coronary magnetic resonance angiography at 3.0-T: a comparative study with X-ray angiography in a single center. *J Am Coll Cardiol* 2009;54:69-76.
43. Piccini D, Monney P, Sierro C, Coppo S, Bonanno G, van Heeswijk RB, et al. Respiratory self-navigated postcontrast whole-heart coronary MR angiography: initial experience in patients. *Radiology* 2014;270:378-386.
 44. Ginami G, Bonanno G, Schwitler J, Stuber M, Piccini D. An iterative approach to respiratory self-navigated whole-heart coronary MR significantly improves image quality in a preliminary patient study. *Magn Reson Med* 2016;75:1594-1604.
 45. Henningsson M, Koken P, Stehning C, Razavi R, Prieto C, Botnar RM. Whole-heart coronary MR angiography with 2D self-navigated image reconstruction. *Magn Reson Med* 2012;67:437-445.
 46. Henningsson M, Smerk J, Razavi R, Botnar RM. Prospective respiratory motion correction for coronary MR angiography using a 2D image navigator. *Magn Reson Med* 2013;69:486-494.
 47. Moghari MH, Roujol S, Henningsson M, Kissinger KV, Annes D, Nezafat R, et al. Three-dimensional heart locator for whole-heart coronary magnetic resonance angiography. *Magn Reson Med* 2014;71:2118-2126.
 48. Prieto C, Doneva M, Usman M, Henningsson M, Greil G, Schaeffter T, et al. Highly efficient respiratory motion compensated free-breathing coronary MRA using golden-step Cartesian acquisition. *J Magn Reson Imaging* 2015;41:738-746.
 49. Aitken AP, Henningsson M, Botnar RM, Schaeffter T, Prieto C. 100% Efficient three-dimensional coronary MR angiography with two-dimensional beat-to-beat translational and bin-to-bin affine motion correction. *Magn Reson Med* 2015;74:756-764.
 50. Lustig M, Donoho D, Pauly JM. Sparse MRI: the application of compressed sensing for rapid MR imaging. *Magn Reson Med* 2007;58:1182-1195.
 51. Pang J, Bhat H, Sharif B, Fan Z, Thomson LE, LaBounty T, et al. Whole-heart coronary MRA with 100% respiratory gating efficiency: self-navigated three-dimensional retrospective image-based motion correction (TRIM). *Magn Reson Med* 2014;71:67-74.
 52. Akçakaya M, Rayatzadeh H, Basha TA, Hong SN, Chan RH, Kissinger KV, et al. Accelerated late gadolinium enhancement cardiac MR imaging with isotropic spatial resolution using compressed sensing: initial experience. *Radiology* 2012;264:691-699.
 53. Akçakaya M, Basha TA, Chan RH, Manning WJ, Nezafat R. Accelerated isotropic sub-millimeter whole-heart coronary MRI: compressed sensing versus parallel imaging. *Magn Reson Med* 2014;71:815-822.
 54. Coppo S, Piccini D, Bonanno G, Chaptinel J, Vincenti G, Feliciano H, et al. Free-running 4D whole-heart self-navigated golden angle MRI: initial results. *Magn Reson Med* 2015;74:1306-1316.
 55. Bunce NH, Lorenz CH, Keegan J, Lesser J, Reyes EM, Firmin DN, et al. Coronary artery anomalies: assessment with free-breathing three-dimensional coronary MR angiography. *Radiology* 2003;227:201-208.
 56. McConnell MV, Ganz P, Selwyn AP, Li W, Edelman RR, Manning WJ. Identification of anomalous coronary arteries and their anatomic course by magnetic resonance coronary angiography. *Circulation* 1995;92:3158-3162.
 57. Taylor AM, Thorne SA, Rubens MB, Jhooti P, Keegan J, Gatehouse PD, et al. Coronary artery imaging in grown up congenital heart disease: complementary role of magnetic resonance and X-ray coronary angiography. *Circulation* 2000;101:1670-1678.
 58. Makino N, Nakamura Y, Yashiro M, Ae R, Tsuboi S, Aoyama Y, et al. Descriptive epidemiology of Kawasaki disease in Japan, 2011-2012: from the results of the 22nd nationwide survey. *J Epidemiol* 2015;25:239-245.
 59. Kato H, Sugimura T, Akagi T, Sato N, Hashino K, Maeno Y, et al. Long-term consequences of Kawasaki disease. A 10- to 21-year follow-up study of 594 patients. *Circulation* 1996;94:1379-1385.
 60. Greil GF, Stuber M, Botnar RM, Kissinger KV, Geva T, Newburger JW, et al. Coronary magnetic resonance angiography in adolescents and young adults with Kawasaki disease. *Circulation* 2002;105:908-911.
 61. Mavrogeni S, Papadopoulos G, Douskou M, Kaklis S, Seimenis I, Baras P, et al. Magnetic resonance angiography is equivalent to X-ray coronary angiography for the evaluation of coronary arteries in Kawasaki disease. *J Am Coll Cardiol* 2004;43:649-652.
 62. Kim WY, Danias PG, Stuber M, Flamm SD, Plein S, Nagel E, et al. Coronary magnetic resonance angiography for the detection of coronary stenoses. *N Engl J Med* 2001;345:1863-1869.
 63. Jahnke C, Paetsch I, Schnackenburg B, Bornstedt A, Gebker R, Fleck E, et al. Coronary MR angiography with steady-state free precession: individually adapted breath-hold technique versus free-breathing technique. *Radiology* 2004;232:669-676.
 64. Kato S, Kitagawa K, Ishida N, Ishida M, Nagata M, Ichikawa Y, et al. Assessment of coronary artery disease using magnetic resonance coronary angiography: a national multicenter trial. *J Am Coll Cardiol* 2010;56:983-991.
 65. Miller JM, Rochitte CE, Dewey M, Arbab-Zadeh A, Niinuma H, Gottlieb I, et al. Diagnostic performance of coronary angiography by 64-row CT. *N Engl J Med* 2008;359:2324-2336.
 66. Yonezawa M, Nagata M, Kitagawa K, Kato S, Yoon Y, Nakajima H, et al. Quantitative analysis of 1.5-T whole-heart coronary MR angiograms obtained with 32-channel cardiac coils: a comparison with conventional quantitative coronary angiography. *Radiology* 2014;271:356-364.
 67. Kim SM, Choi JH, Choe YH. Coronary artery total occlusion: MR angiographic imaging findings and success rates of percutaneous coronary intervention according to intraluminal signal intensity patterns. *Radiology* 2016;279:84-92.
 68. Bettencourt N, Ferreira N, Chiribiri A, Schuster A, Sampaio F, Santos L, et al. Additive value of magnetic resonance coronary angiography in a comprehensive cardiac magnetic resonance stress-rest protocol for detection of functionally significant coronary artery disease: a pilot study. *Circ Cardiovasc Imaging* 2013;6:730-738.
 69. Klein C, Gebker R, Kokocinski T, Dreyse S, Schnackenburg B, Fleck E, et al. Combined magnetic resonance coronary artery imaging, myocardial perfusion and late gadolinium enhancement in patients with suspected coronary artery disease. *J Cardiovasc Magn Reson* 2008;10:45.
 70. Ripley DP, Motwani M, Brown JM, Nixon J, Everett CC, Bijsterveld P, et al. Individual component analysis of the multi-parametric cardiovascular magnetic resonance protocol in the CE-MARC trial. *J Cardiovasc Magn Reson* 2015;17:59.
 71. Heer T, Reiter S, Höfling B, Pilz G. Diagnostic performance of non-contrast-enhanced whole-heart magnetic resonance coronary angiography in combination with adenosine stress perfusion cardiac magnetic resonance imaging. *Am Heart J* 2013;166:999-1009.
 72. Yoon YE, Kitagawa K, Kato S, Ishida M, Nakajima H, Kurita T, et al. Prognostic value of coronary magnetic resonance angiography for prediction of cardiac events in patients with suspected coronary artery disease. *J Am Coll Cardiol* 2012;60:2316-2322.
 73. Kim WY, Astrup AS, Stuber M, Tarnow L, Falk E, Botnar RM, et al. Sub-clinical coronary and aortic atherosclerosis detected by magnetic resonance imaging in type 1 diabetes with and without diabetic nephropathy. *Circulation* 2007;115:228-235.
 74. Kim WY, Stuber M, Börnert P, Kissinger KV, Manning WJ, Botnar RM. Three-dimensional black-blood cardiac magnetic resonance coronary vessel wall imaging detects positive arterial remodeling in patients with non-significant coronary artery disease. *Circulation* 2002;106:296-299.
 75. Makowski MR, Henningsson M, Spuentrup E, Kim WY, Maintz D, Manning WJ, et al. Characterization of coronary atherosclerosis by magnetic resonance imaging. *Circulation* 2013;128:1244-1255.
 76. Jansen CH, Perera D, Makowski MR, Wiethoff AJ, Phinikaridou A, Razavi RM, et al. Detection of intracoronary thrombus by magnetic resonance imaging in patients with acute myocardial infarction. *Circulation* 2011;124:416-424.
 77. Kawasaki T, Koga S, Koga N, Noguchi T, Tanaka H, Koga H, et al. Characterization of hyperintense plaque with noncontrast T(1)-weighted cardiac magnetic resonance coronary plaque imaging: comparison with multislice computed tomography and intravascular ultrasound. *JACC*

- Cardiovasc Imaging 2009;2:720-728.
78. Noguchi T, Kawasaki T, Tanaka A, Yasuda S, Goto Y, Ishihara M, et al. High-intensity signals in coronary plaques on noncontrast T1-weighted magnetic resonance imaging as a novel determinant of coronary events. *J Am Coll Cardiol* 2014;63:989-999.
 79. Noguchi T, Tanaka A, Kawasaki T, Goto Y, Morita Y, Asaumi Y, et al. Effect of intensive statin therapy on coronary high-intensity plaques detected by noncontrast T1-weighted imaging: the AQUAMARINE pilot study. *J Am Coll Cardiol* 2015;66:245-256.
 80. Ibrahim T, Makowski MR, Jankauskas A, Maintz D, Karch M, Schachoff S, et al. Serial contrast-enhanced cardiac magnetic resonance imaging demonstrates regression of hyperenhancement within the coronary artery wall in patients after acute myocardial infarction. *JACC Cardiovasc Imaging* 2009;2:580-588.
 81. Yeon SB, Sabir A, Clouse M, Martinezclark PO, Peters DC, Hauser TH, et al. Delayed-enhancement cardiovascular magnetic resonance coronary artery wall imaging: comparison with multislice computed tomography and quantitative coronary angiography. *J Am Coll Cardiol* 2007;50:441-447.
 82. Kooi ME, Cappendijk VC, Cleutjens KB, Kessels AG, Kitslaar PJ, Borgers M, et al. Accumulation of ultrasmall superparamagnetic particles of iron oxide in human atherosclerotic plaques can be detected by in vivo magnetic resonance imaging. *Circulation* 2003;107:2453-2458.
 83. Lobbes MB, Miserus RJ, Heeneman S, Passos VL, Mutsaers PH, Debernardi N, et al. Atherosclerosis: contrast-enhanced MR imaging of vessel wall in rabbit model--comparison of gadofosveset and gadopentetate dimeglumine. *Radiology* 2009;250:682-691.
 84. Phinikaridou A, Andia ME, Protti A, Indermuehle A, Shah A, Smith A, et al. Noninvasive magnetic resonance imaging evaluation of endothelial permeability in murine atherosclerosis using an albumin-binding contrast agent. *Circulation* 2012;126:707-719.
 85. Tang TY, Howarth SP, Miller SR, Graves MJ, Patterson AJ, U-King-Im JM, et al. The ATHEROMA (Atorvastatin Therapy: Effects on Reduction of Macrophage Activity) Study. Evaluation using ultrasmall superparamagnetic iron oxide-enhanced magnetic resonance imaging in carotid disease. *J Am Coll Cardiol* 2009;53:2039-2050.